

INFLUENCE OF GAS DETONATION SPRAYING PARAMETERS ON THE GEOMETRICAL STRUCTURE OF FE-AL INTERMETALLIC PROTECTIVE COATINGS*

*Tomasz Chrostek*¹, *Mirosław Bramowicz*², *Kazimierz Rychlik*³,
*Adam Wojtkowiak*⁴, *Cezary Senderowski*⁵

¹ORCID: 0000-0002-6516-8192

Department of Materials and Machine Technology
University of Warmia and Mazury in Olsztyn

²ORCID: 0000-0002-7716-544X

Department of Materials and Machine Technology
University of Warmia and Mazury in Olsztyn

³ORCID: 0000-0003-2978-4681

Research Network LUKASIEWICZ
Institute of Mechanized Construction and Rock Mining, Warsaw

⁴Department of Materials and Machine Technology
University of Warmia and Mazury in Olsztyn

⁵ORCID: 0000-0002-0331-3702

Department of Materials and Machine Technology
University of Warmia and Mazury in Olsztyn

University of Warmia and Mazury in Olsztyn Received 7 October 2019,
accepted 29 January 2020, available online 31 January 2020.

Key words: GDS, Detonation Gas Spraying, Fe-Al, intermetallic alloys, fractal analysis, RMS.

Abstract

The paper presents the results of an analysis of the geometrical structure of Fe-Al intermetallic protective coatings sprayed under specified gun detonation spraying (GDS) conditions. Two barrel lengths, two powder injection positions (PIP) at the moment of spark detonation, and two numbers of GDS shots with 6.66 Hz frequency were applied as variable parameters in the GDS process.

Correspondence: Tomasz Chrostek, Katedra Technologii Materiałów i Maszyn, Wydział Nauk Technicznych, Uniwersytet Warmińsko-Mazurski, ul. Oczapowskiego 11/E27, 10-719 Olsztyn, phone: +48 89 5233855, e-mail: tomasz.chrostek@uwm.edu.pl.

* This study was financed as part of project No. 2015/19 / B / ST8 / 02000 of the Polish National Science Center of Poland.

Surface profile measurements were conducted by contact profilometry with the use of the TOPO-01 system and the Mitutoyo SJ 210 profilometer. The measured parameters were used to analyze surface topography in two-dimensional (2D) and three-dimensional (3D) systems. It was assumed that roughness can be regarded as a non-stationary parameter of variance in surface amplitude which is highly dependent on the sampling rate and spraying distance. Therefore, changes in surface amplitude parameters and functional properties were analyzed across segments with a length (ln) of 1.25, 4 and 12.5 mm. The development of the geometric structure of the surface was analyzed with the RMS (Root Mean Square) fractal method, and the geometric structure of the surface stretched by several orders of magnitude was evaluated based on the correlation between roughness (Rq), segment length (ln) and fractal dimension (D). The RMS method and the calculated fractal dimension (D) supported the characterization of the geometric structure of intermetallic Fe-Al protective coatings subjected to GDS under the specified process conditions based on the roughness profiles of surface segments with a different length (ln).

Introduction

Intermetallic alloys based on ordered intermetallic phases belong to a group of innovative engineering materials used in industry. This group includes alloys from the Fe-Al equilibrium system which are functional materials with unique performance properties that can be applied as protective coatings in high-temperature environments (BYSTRZYCKI et al. 1996). Intermetallic alloys are particularly suited for use as heat-resistant construction materials on account of their resistance to high temperature corrosion in aggressive sulfide and chloride environments. However, high brittleness and the problems associated with the production of solid alloys with a fine-grained structure that are free of structural defects (JASIONOWSKI et al. 2011, 2012, NIEWIELKI, JABŁOŃSKA 2007) pose a major limitation to the widespread use of intermetallic alloys.

Despite their weaknesses, Fe-Al intermetallic alloys have a number of important functional properties, including excellent oxidation resistance, structural and chemical stability at elevated temperatures and, equally importantly, the ability to form Al_2O_3 oxides on the surface. A tight protective oxide layer increases resistance to oxidation, carburization and sulfation, which renders iron-aluminum intermetallics suitable for the production of components that operate in an aggressive gas environment. The above was confirmed by studies where Fe-Al intermetallic alloys with 28-Fe at% Al and 35-Fe at% Al were significantly more resistant to heat than the components made of commercial chromium-nickel steel (Fe-25Cr-20Ni) and chromium-aluminum (19-Fe at% and 12-Cr at% Al). FeAl alloys are used in aluminum extrusion and in the production of grate bars that are resistant to furnace operations at roughly 1,000°C. They are also applied in the production of intermetallic (FeAl) pallets and stands in both heat and chemical treatment furnaces, furnace rails and rollers for transporting hot-rolled steel sheets (BYSTRZYCKI et al. 1996, JASIONOWSKI et al. 2011, NIEWIELKI, JABŁOŃSKA 2007, SCHNEIBEL et al. 2005). Intermetallic

alloys are also relatively cheaper than other groups of heat-resistant materials (JASIONOWSKI et al. 2011, NIEWIELKI, JABŁOŃSKA 2007).

Conventional methods of producing Fe-Al intermetals, such as melting or casting, can be problematic. Therefore, thermal spraying methods that produce coatings with potentially promising properties and are characterized by adhesive bonding to the base material are becoming increasingly popular. Several thermal spraying methods produce coatings with different properties and applications, depending on the type of spraying equipment and process parameters. Many years of research and industrial experience have led to the development of technologies that differ in the generation and acceleration of the metallizing stream containing particles of the coating material. Coatings are generally produced with the involvement of the available spray metallization methods, including (ASSADI 2016, CINCA, GUILMANY 2012, CHEN et al. 2009, HEJWOWSKI 2013, MUŚALEK et al. 2010, SENDEROWSKI et al. 2011, SENDEROWSKI 2015, SZULC 2013, XU et al. 2004, YAN et al. 2012, ŻÓRAWSKI 2010):

- a) High Velocity Arc Spraying (HVAS),
- b) Atmospheric Plasma Spraying (APS),
- c) High Velocity Oxygen Fuel (HVOF),
- d) Cold Spraying,
- e) Gas Detonation Spraying (GDS).

Thermal spraying technologies are usually quite complex processes whose parameters affect coating performance regardless of the applied method. All thermal spraying methods are characterized by specific temperature and velocity of the metallizing stream which determine the kinetic energy of powder charge particles that form the coating. These methods support the production of coatings with the required properties, such as porosity, hardness, adhesive strength, natural stress distribution and oxidation state, within a short period of time (BOJAR et al. 1996).

Gun detonation spraying (GDS) is a popular coating method, but the technological requirements during the supersonic flow of a two-phase (gas-powder) metallization stream and the formation of a layered coating structure with oxide phases formed in-situ during GDS are still in the research phase (SENDEROWSKI et al. 2011).

The GDS process produces geometrically uniform coatings with an axially symmetric thickness distribution. This effect can be achieved by monitoring the entire spraying process and its repeatability in each working cycle. Coating geometry is generally determined by the speed with which powder particles collide with the base material and the thermal energy released during this event (SENDEROWSKI et al. 2011). The aim of this study was to determine the effect of the length of the GDS gun barrel on the geometry, performance, functional properties, including roughness, and fractal properties of coatings.

Materials and Methods

Four coatings produced by gun detonation spraying of intermetallic powder material based on the FeAl phase matrix with 40% aluminum content were tested. The powder with 5-40 μm particle size was manufactured by the Vacuum Inert Gas Atomization (VIGA) method. The substrate was 15 HM boiler steel measuring 50×50×5 mm (Fig. 1). The surface layer of the substrate material was blasted with alumina before spraying. Circular coatings were obtained by placing the substrate material in a stationary position relative to the barrel outlet.

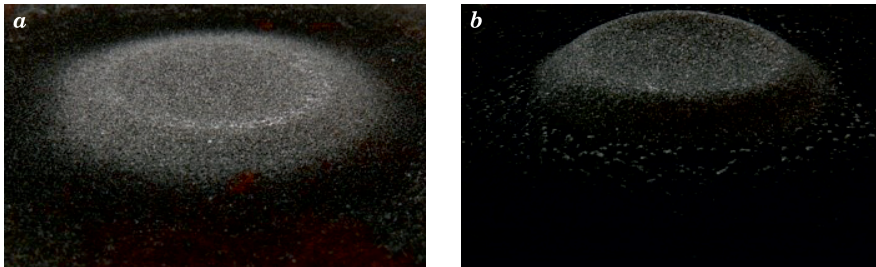


Fig. 1. FeAl coatings sprayed onto 15 HM boiler steel by the GDS method with: *a* – 100, *b* – 400 shots, without changing the position of the barrel relative to the base material

Intermetallic materials based on the FeAl phase are characterized by considerable resistance to high temperatures in chemically aggressive environments, stable and ordered structure up to around 1,100°C, and significant resistance to both abrasive and erosive tribological wear (CHROSTEK et al. 2018). The GDS process was carried at the Paton Institute in Kiev with the use of the Perun-S gun with different spraying parameters (Tab. 1).

Table 1

GDS parameters					
Fe40Al10.05Zr at% powder +50 ppm B				Granulation 5–40 μm	
Oxygen-fuel mixture				C ₃ H ₈ – 0.45 m ³ /h	
				O ₂ – 1.52 m ³ /h	
				air – 0.65 m ³ /h	
Air flow rate				0.4 m ³ /h	
Spraying frequency				<i>f</i> = 6.66 Hz	
Coating	spraying distance <i>L</i> [mm]	barrel length [mm]	PIP* [mm]	number of GDS shots	coating thickness [mm]
1	110	590	412.5	400	2.91
2			274.5	100	0.86
3		1,090	412.5	100	0.56
4			274.5	400	1.13

* powder injection position – location of powder in the barrel at the time of detonation

Different powder injection positions (PIP), i.e. powder locations in the barrel at the moment of ignition initiation, a different number of shots, and different barrel lengths were applied during the experiment. Coatings were formed through cyclical gradient concentration deposition at a frequency of 6.66 Hz, with a constant composition of the explosive mixture (propane) as the working gas. The distance between the barrel ($\text{\O}23$ mm inner diameter) and the sprayed substrate was $L = 110$ mm.

Surface profilometric measurements were carried out by the contact method with the TOPO-01 modular measuring system which measures shape contours on flat cylindrical external and internal surfaces. The system's high accuracy and broad measuring range support a comprehensive characterization of the surface profile based on 2D measurements of roughness, wave and shape. Stereometric 3D measurements can be performed by moving the analyzed object in the Y-axis on a table. The measuring head has a diamond tip with a $2\ \mu\text{m}$ radius and a 60° cone angle (Fig. 2).

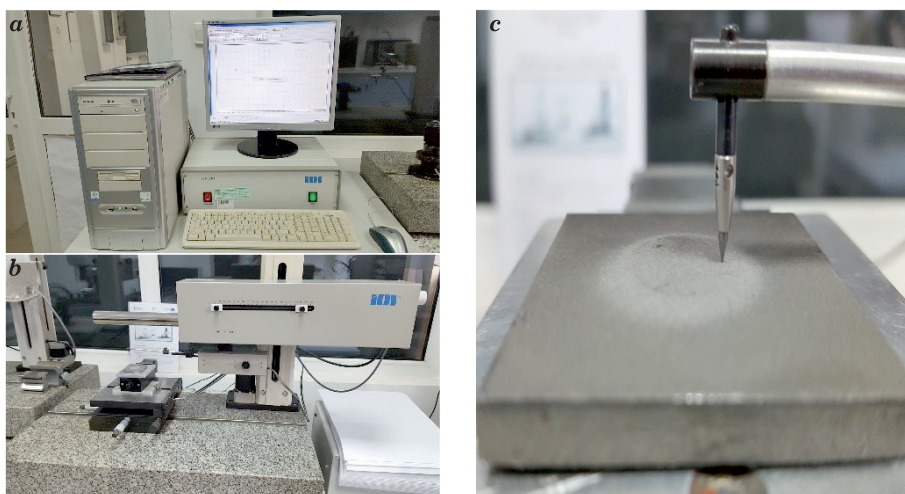


Fig. 2. TOPO-01 system for measuring surface topography: *a* – computer with the TOPO-01 control module, *b* – PG 2/200 shape-maker for 3D stereometric measurements, *c* – measuring head

Coating surfaces were analyzed in 26 passes at a speed of $1\ \text{mm/s}$ in increments of $1\ \text{mm}$. The measured area was $25 \times 25\ \text{mm}$. The measured parameters are given in Table 2.

Surface roughness tests were carried out using the Mitutoyo SJ-210 contact device. The measuring head has a cone-shaped diamond blade with an angle of 60° and a tip radius of $2\ \mu\text{m}$. The surface mapping range is $360\ \mu\text{m}$ (from -200 to $+160\ \mu\text{m}$).

Table 2

Coating surface topography	
X-axis feed	25 mm
Y-axis feed	25 mm
Feed speed	1 mm/s
Number of passes	26
Stroke in the Y-axis	every 1 mm
Straightness	0.3 $\mu\text{m}/25\text{ mm}$
Resolution	0.1 μm
Maximum head load (auto)	15 N

Roughness was regarded a non-stationary parameter of variance in surface amplitude which is determined by sampling density and the length of the measuring segment. Changes in amplitude and the functional properties of the tested surface were analyzed across segments with a length (ln) of 1.25, 4 and 12.5 mm.

Roughness parameters denote the statistical distribution of points across the analyzed segment of the tested surface (SAYLES, THOMAS 1978). According to the cited authors, surface height variance (σ^2) is proportional to sampling length, which is described by the below relationship (1):

$$\sigma^2 \propto L \quad (1)$$

The following relationship (2) was proposed by BERRY and HANNAY (1978) to describe variance as a function of scale:

$$\sigma^2 \propto L^H \quad (2)$$

For this reason, the root mean square (RMS) method (BHUSHAN 1999, MAINSAH et al. 2001, AUE 1997) was applied in this study. The RMS approach is a fractal method that provides information about the degree of surface development. It is used to describe the geometric structure of a surface stretched by several orders of magnitude. In this experiment, the fractal dimension (D) was calculated to describe the surface profile across the measured segment with a length (ln) of 1.25 to 12.5 mm. In two-dimensional systems such as surface profiles, D ranges from 1 to 2, where $D = 1$ denotes a straight line, and $D = 2$ denotes an extremely developed surface that consists of an infinite number of sections. Equation (2) takes on the following form (3) when it is applied to roughness Rq based on the relationship between the fractal dimension and the Hurst parameter (H):

$$Rq \propto L^{\frac{2-D}{2}} \quad (3)$$

Three basic waveforms are obtained by plotting the relationship (3) in a logarithmic system (Fig. 3).

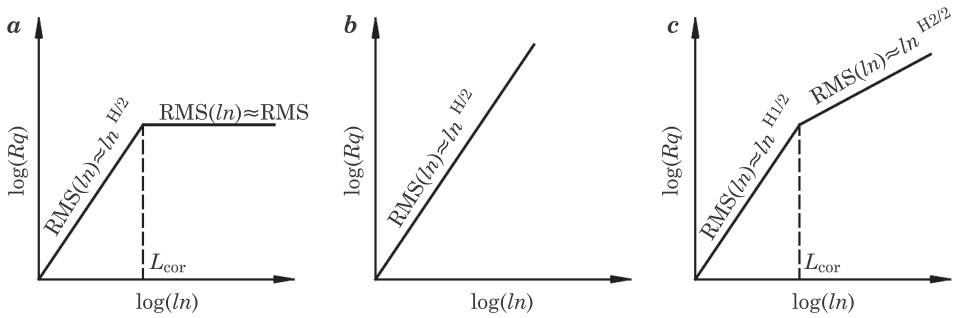
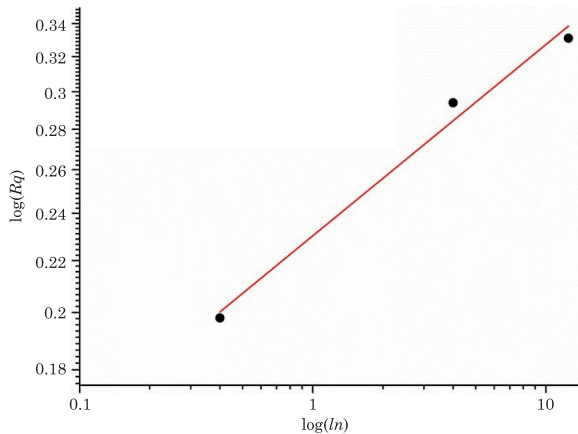


Fig. 3. Basic relationships of $Rq = f(L)$

Source: based on AUE (1997).

In Figure 3a, the surface topography of the measured segment with length $< L_{cor}$ is governed by scaling laws. When the above length is exceeded, roughness becomes a stationary process, and Rq is no longer determined by the length of the measured segment. Such surfaces can be described by the fractal dimension D in the range of $L < L_{cor}$, where the value of D is related to the exponent: $\frac{H}{2} = 2 - D$. The surface presented in Figure 3b exhibits fractal properties across the entire range of the measurements, whereas the surface in Figure 3c has



equation	$y = a + b \cdot x$		
weight	no weighting		
residual sum of squares	3.22079E-4		
pearson's r	0.99409		
adj. R-Square	0.97641		
		value	standard error
B	intercept	-0.63787	0.01263
	slope	0.15254	0.01666

Fig. 4. The application of the RMS method in profilometric measurements

bifractal properties. These type of structures correspond to cluster structures, where cluster surface is characterized up to the length L_{cor} , and the structure of cluster arrangement is characterized for $L > L_{\text{cor}}$.

In this study, the RMS method was used in profilometric measurements. Points with coordinates (ln, Rq) were plotted in the log-log system, and point relationships were approximated by the power function $y = ax^b$ whose logarithmic form is a linear function with a directional coefficient $1 - \frac{D}{2}$. An exemplary $\log(Rq) = f(\log(ln))$ relationship is shown in Figure 4.

The RMS method supported the description of spray-coated surfaces across the measured sections with a length of 1.25 to 12.5 mm and provided information about surface development.

Results and Discussion

The results of the performed analyses were used to generate isometric views and contour maps describing the analyzed surface and the parameters characterizing the three-dimensional surface of the coatings. Geometrically homogeneous coatings with an estimated diameter of 25 mm, whose thickness was determined by the applied spraying parameters, were formed by 100 and 400 cyclically fired shots with fixed barrel position relative to the sprayed substrate. An analysis of the obtained profilographs indicates that spraying parameters significantly influenced the shape, flat dimensions and thickness distribution of the sprayed coatings (Fig. 5). Regardless of the number of fired GDS shots,

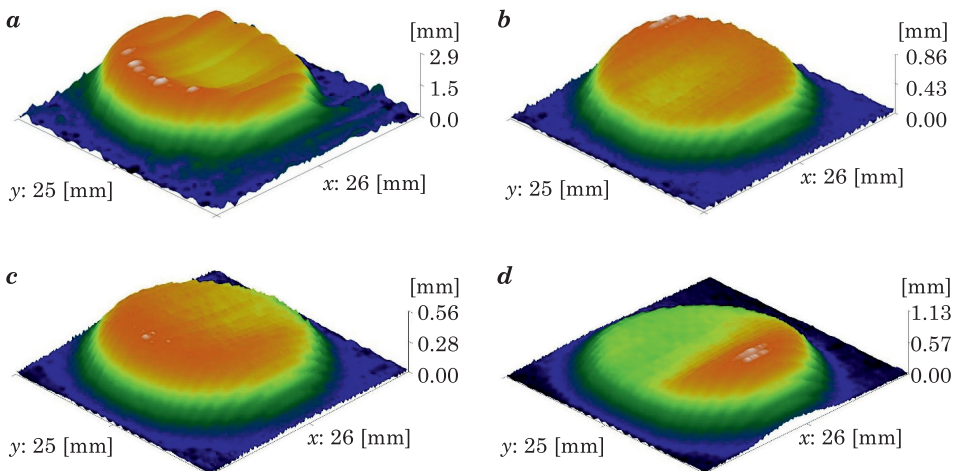


Fig. 5. Isometric view of Fe-Al coatings after GDS spraying – coating numbers correspond to the data in Table 1: *a* – 1, *b* – 2, *c* – 3, *d* – 4

barrel length exerted the greatest impact on coating thickness. The coatings produced with the use of a shorter barrel (590 mm) were much thicker than those formed with a longer barrel (1,090 mm).

Depending on the applied spraying parameters, the maximum thickness zone of a “static” coating is geometrically shifted by around 6 to 8 mm relative to the barrel axis (Fig. 6). The axially asymmetric distribution of coating thickness indicates that:

- the stream of detonation products entered into dynamic interactions with the substrate and powder particles transported by the stream,
- powder particles were unevenly distributed in the stream of detonation products, which lead to uneven heating of particles at different flow rates,
- more dispersed powder particles (shifted from the axis of the detonation stream) are less deformed after colliding with the substrate.

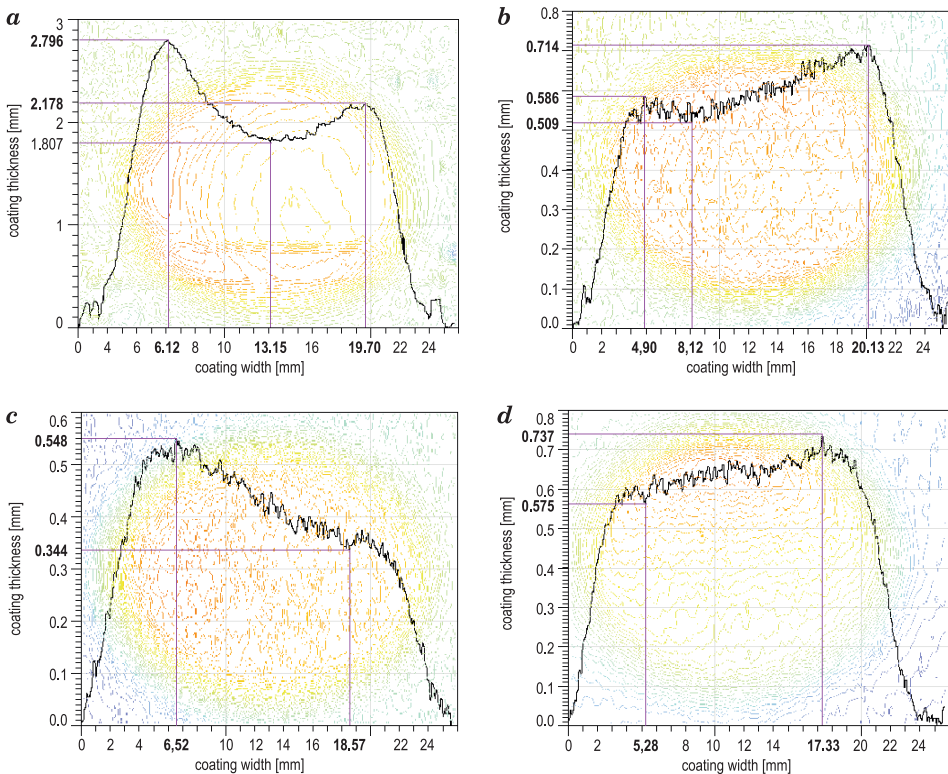
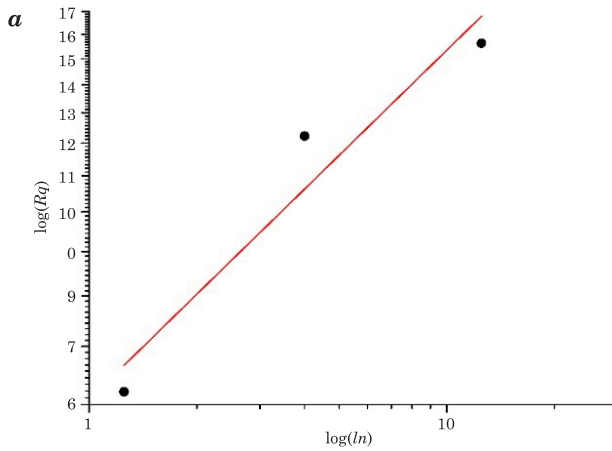
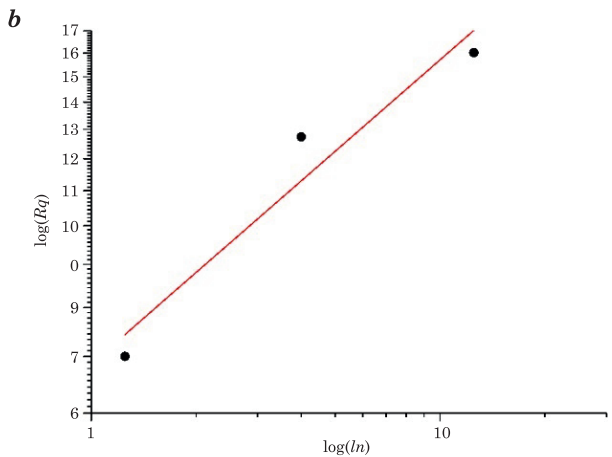


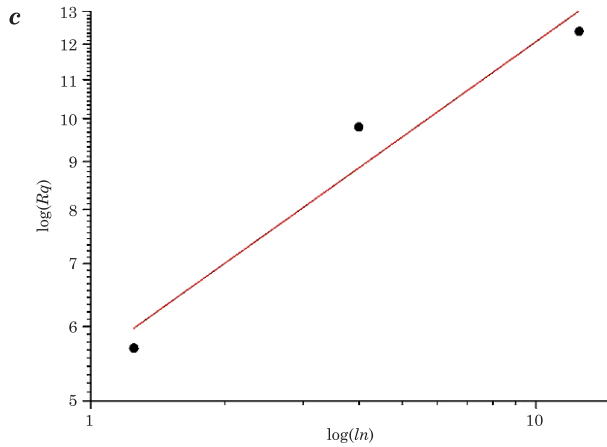
Fig. 6. Thickness distribution of Fe-Al coatings across the cross-sectional diameter and contour maps – coating numbers correspond to the data in Table 1: *a* – 1, *b* – 2, *c* – 3, *d* – 4



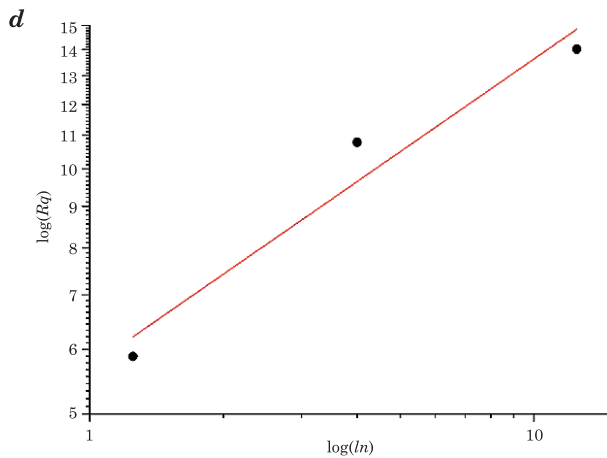
equation	$y = a + b \cdot x$		
weight	no weighting		
residual sum of squares	0.00561		
pearson's r	0.9669		
adj. R-Square	0.8698		
		value	standard error
<i>B</i>	intercept	0.7842	0.07678
	slope	0.4016	0.10596



equation	$y = a + b \cdot x$		
weight	no weighting		
residual sum of squares	0.00403		
pearson's r	0.96988		
adj. R-Square	0.88134		
		value	standard error
<i>B</i>	intercept	0.8362	0.06548
	slope	0.3598	0.09037



equation	$y = a + b \cdot x$		
weight	no weighting		
residual sum of squares	0.00283		
pearson's r	0.9761		
adj. R-Square	0.9056		
		value	standard error
<i>B</i>	intercept	0.7437	0.05455
	slope	0.3382	0.07528



equation	$y = a + b \cdot x$		
weight	no weighting		
residual sum of squares	0.00348		
pearson's r	0.9764		
adj. R-Square	0.9069		
		value	standard error
<i>B</i>	intercept	0.7570	0.06043
	slope	0.3776	0.0834

Fig. 7. Root mean square deviation (RMS) of roughness as a function of the length of the scanned area (*ln*) – coating numbers correspond to the data in Table 1: *a* – 1, *b* – 2, *c* – 3, *d* – 4

Surface roughness is a non-stationary process, and roughness parameters indicate the extent to which roughness is influenced by sampling density and the length of the measured segment. The formed coatings had irregular shape; therefore, roughness was measured in the center. The root mean square deviation of roughness as a function of the scanned area, plotted in a logarithmic coordinate system, is presented in Figure 7. Roughness parameters denote the static distribution of points on the tested surfaces. An analysis of the obtained results revealed that the number of GDS shots exerted the greatest influence on the degree of surface development. The degree of surface development decreased with a rise in the number of GDS shots (Tab. 3).

Table 3

RMS test results				
Coating	Length L_n [mm] of the scanned segment	Root mean square deviation R_q [um]	Slope a	Fractal dimension D
1^a	1.25	6.2072	0.4016	1.1968
	4	12.2248		
	12.5	15.6286		
2^b	1.25	7.0036	0.3598	1.2804
	4	12.7372		
	12.5	16.0178		
3^b	1.25	5.6892	0.3382	1.3236
	4	9.7922		
	12.5	12.3834		
4^a	1.25	5.8858	0.3776	1.2448
	4	10.7782		
	12.5	14.0264		

^a Coating 1 and 4 – 400 GDS shots fired

^b Coating 2 and 3 – 100 GDS shots fired

Conclusions

The described experiment supported the characterization of the geometric structure of the surface of FeAl-type intermetallic protective coatings formed by gun detonation spraying. The study demonstrated that barrel length significantly affected coating thickness. Regardless of the number of fired GDS shots, the thickest coatings were formed when barrel length was 590 mm.

The RMS method can be used to confirm fractal surface properties. Coating surfaces are governed by scaling laws and are statistically self-similar (each segment of the profile on a given scale is similar to the whole) within the measured

range of 1.25 to 12.5 mm. The degree of surface development decreased with a rise in the number of fired shots. The above can probably be attributed to shock-wave compaction effects during cyclic operation of the GDS gun, which acts a precursor of gaseous detonation combustion products that transport powder particles of FeAl coating.

References

- ASSADI H., KREYE H., GARTNER F., KLASSEN T. 2016. *Cold spraying – A materials perspective*. Acta Materialia, 116: 382-407.
- AUE J.-J. 1997. *Fractals and fracture: structure-property relationship of highly porous ceramics*. Dissertations of University of Groningen.
- BERRY M.V., HANNAY J.H. 1978. *Topography of Random Surfaces*. Nature, 271: 573.
- BHUSHAN B. 1999. *Introduction – Measurement Techniques and Applications*. Handbook of Micro/Nanotribology. Ed. Bharat Bhushan. CRC Press LLC, Boca Raton.
- BOJAR Z., KOMOREK Z., DUREJKO T. 1996. *Struktura i właściwości intermetalicznych powłok ochronnych otrzymanych metodą detonacyjną*. Solidification of Metals and Alloys, 27: 115-119.
- BYSTRZYCKI J., VARIN R.A., BOJAR Z. 1996. *Postępy w badaniach stopów na bazie uporządkowanych faz międzymetalicznych z udziałem aluminium*. Inżynieria Materiałowa, 5: 137-149.
- CINCA N., GUILLEMANY J.M. 2012. *Thermal spraying of transition metal aluminides: An overview*. Intermetallics, 24: 60-72.
- CHEN Y., LIANG X., WEI S., LIU Y., XU B. 2009. *Heat treatment induced intermetallic phase transition of arc-sprayed coating prepared by the wires combination of aluminum-cathode and steel-anode*. Applied Surface Science, 255(19): 8299-8304.
- CHROSTEK T., RYCHLIK K., BRAMOWICZ M., SENDEROWSKI C. 2018. *Functional and fractal properties of Fe-Al coatings after gas detonation spraying (GDS)*. Archives of Metallurgy and Materials, 63(4): 1991-1997.
- HEJWOWSKI T. 2013. *Nowoczesne powłoki nakładane cieplnie odporne na zużycie ścierne i erozyjne*. Monografie, Politechnika Lubelska, Lublin.
- JASIONOWSKI R., PRZETAKIEWICZ W., ZASADA D. 2011. *The effect of structure on the cavitation wear of Fe-Al intermetallic phase-based alloys with cubic lattice*. Archives of Foundry Engineering, 11(2): 97-102.
- JASIONOWSKI R., BRYLL K., GRABIAN J. 2012. *Badanie właściwości tribologicznych intermetali*. Archives of Foundry Engineering, 12: 87-90.
- MAINSAH E., GREENWOOD J.A., CHETWYND D.G. 2001. *Metrology and Properties of Engineering Surfaces*. Kluwer Academic Publishers.
- MUŚALEK R., KOVARIK O., SKIBA T., HAUSILD P., KARLIK M., COLMENARES-ANGULO J. 2010. *Fatigue properties of Fe-Al intermetallic coatings prepared by plasma spraying*. Intermetallics, 18: 1415-1418.
- NIWIELKI G., JABŁOŃSKA M. 2007. *Charakterystyka i zastosowanie intermetali z układu Fe-Al*. Inżynieria Materiałowa, 2: 43-47.
- SAYLES R.S., THOMAS T.R. 1978. *Surface Topography as a Nonstationary Random Process*. Nature, 271: 431-434.
- SCHNEIBEL J.H., RITCHIE R.O., KRUZIC J.J., TORTORELLI P.F. 2005. *Optimization of Mo-Si-B Intermetallic Alloys*. Metallurgical and Materials Transaction A, 36(3): 525-531.
- SENDEROWSKI C., ASTACHOV E., BOJAR Z., BORISOV Y. 2011. *Elementarne mechanizmy formowania powłoki intermetalicznej Fe-Al podczas natryskiwania gazodetonacyjnego*. Inżynieria Materiałowa, 4: 719-723.

- SENDEROWSKI C. 2015. *Żelazowo-aluminiowe intermetaliczne systemy powłokowe uzyskiwane z naddźwiękowego strumienia metalizacyjnego*. Bel Studio Sp. z o.o., Warszawa.
- SZULC T. 2013. *Notatki z historii natryskiwania termicznego*. Przegląd Spawalnictwa, 85(6): 76-83.
- XU B., ZHU Z., MA S., ZHANG W., LIU W. 2004. *Sliding wear behavior of Fe-Al and Fe-Al/WC coatings prepared by high velocity arc spraying*. Wear, 257(11): 1089-1095.
- YAN D., YANG Y., DONG Y., CHEN X., WANG L., ZHANG J. 2012. *Phase transitions of plasma sprayed FeAl intermetallic coating during corrosion in molten zinc at 640°C*. Intermetallics, 22: 160-165.
- ŻÓRAWSKI W. 2010. *Właściwości powłok natryskanych plazmowo i HVOF*. Tribologia, 6: 319-327.